12^{th} International Conference on Fracture Mechanics of Concrete and Concrete Structures
FraMCoS-12
B.L.A. Pichler, Ch. Hellmich, P. Preinstorfer (Eds)

https://doi.org/10.21012/FC12.1147
MS04:3

A PHASE FIELD DAMAGE MODEL FOR MICROPOLAR CONTINUUM UNDERGOING FINITE ROTATION: APPLICATION TO CONCRETE

Ved Prakash*, Akash Kumar Behera†,Mohammad Masiur Rahaman† AND Debasish Roy*

* Department of Civil Engineering; Indian Institute of Science
Bengaluru 560012 India
e-mail: vedprakash@iisc.ac.in, royd@iisc.ac.in

†School of Infrastructure, Indian Institute of Technology Bhubaneswar
Odisha 752050, India
e-mail: s21ce09007@iitbbs.ac.in, masiurr@iitbbs.ac.in

Key words: Quasi brittle, Phase field model, Micropolar, Concrete

Abstract. The behaviour of concrete is greatly influenced by its internal composition. Unlike brittle materials, concrete and other quasi-brittle materials have a larger fracture process zone due to the presence of microcracks. Traditional analysis methods may fail to account for the effects of its heterogeneous structure. Experimentally, this heterogeneity results in variabilities in the global response, such as peak load and post-peak behaviour. To address this, we propose a novel cohesive phase field model for analyzing quasi-brittle fractures in concrete, treating the material behaviour as a generalized continuum. This model considers the deformation of the material's internal structure at the continuum level, assuming it can undergo finite rigid rotation, characteristic of a micropolar continuum. This framework can be extended to more complex behaviours such as micro stretch and micromorphic continuum. The model's elastic response is insensitive to the smoothing length scale, which is introduced to approximate the sharp crack topology with a continuous scalar field variable. Our model introduces additional length scales related to bending and torsional rigidity, allowing for a better representation of size-dependent effects in concrete. We demonstrate the impact of various parameters in our formulation on matching experimental data. The variation of these parameters highlights the variations in internal structure, offering insights into how the additional parameters relate to the material's varying internal structure.

1 INTRODUCTION

Concrete is a prevalent material in construction engineering due to its ease of casting and strength development over time through hydration. It is a composite primarily composed of cement, sand, aggregate, and water. Our focus is on hardened concrete, which is considered to be in two phases: mortar and aggregate. In continuum damage models, concrete is typically treated as homogeneous and isotropic. However, variations in the constituent phases lead to differences in the mechanical properties of concrete. The behaviour of aggregates during concrete deformation can significantly influence the overall response, a factor often neglected in traditional continuum models.

One such approach that incorporates the effects of inner structure at the continuum level is the micropolar continuum model [1]. This model introduces additional degrees of freedom in the form of micro rotations alongside the classical translational degrees of freedom. These rotations are attributed to the deforma-

tion of the inner structure, which is assumed to have independent rotations distinct from those captured by the rotation appearing from the polar decomposition of the deformation gradient in classical continuum mechanics. While more general models exist, such as the micro stretch continuum [2], which allows for stretching while maintaining rotational orthogonality, or the micromorphic continuum [3], which allows both stretching and breaking of rotational orthogonality, our study focuses on the micropolar continuum with finite rotation.

To model the degradation mechanism in concrete, we employ the cohesive phase field model (PFM) [4]. The PFM model for fracture is highly popular due to its ability to treat the problem as an energy minimization problem. The crack path emerges as part of the solution to the governing partial differential equation (PDE) in a scalar variable known as the phase field, which ranges continuously from 0 (fully damaged) to 1 (intact). A diffusing length scale is introduced to facilitate the transition from a sharp crack to an intact phase. Specifically, we use the cohesive PFM for the micropolar continuum as proposed by [4] for representing concrete fracture. However, Unlike the cited work, we assume the material can undergo finite rotations rather than infinitesimal ones. The reason is that the presence of a higher gradient near the damaged surface might lead to finite rotation. A key feature of this model is that the elastic response is insensitive to the diffusing length scale in the PFM. However, the length scale must be small enough to resolve the crack.

In this study, we first introduce the governing equations for the PFM applied to a micropolar continuum experiencing finite rotation. We then examine the impact of two additional parameters—micropolar ratio and bending length scale—on the behaviour of a 2D concrete specimen undergoing damage using a specific St. Venant-Kirchhoff type of energy. A micropolar ratio of 0 corresponds to a linear elastic case. In contrast, a ratio of 1 aligns with couple stress theory [5] where the relative rotation between the inner structure and macrostructure vanishes [6]. The bending length scale is associated with rigidity against bending, meaning that a higher bending length scale results in lower microrotation values. After showing the role of various parameters, we conclude the study with a summary and future scope.

2 Formulation

In this section, we introduce the kinematics associated with the micropolar continuum, along with the strain measures and conjugate stresses. We also present the governing equation subsequently.

2.1 Kinematics

Let us consider a solid body undergoing finite deformation. We consider a subset of undeformed configuration denoted by Ω. With the boundary denoted by $\Gamma = \Gamma_d \cup \Gamma_N$. Γ_d and Γ_N correspond to the Dirichlet and Neumann boundary, respectively. Following the standard continuum mechanics, we denote the components of material points in the deformed and undeformed configuration by x_i and X_i, respectively, where $i = 1, 2, 3$. Deformation gradient is defined as $F_{ij} = \frac{\partial x_i}{\partial X_j}$. Let us denote the microrotation tensor by $\hat{R}_{ij}$, we define the strain measures as [7]

$$\hat{E}_{ij} = \hat{R}_{ki} U_{kj} - \delta_{ij} \tag{1}$$

and

$$\hat{K}_{ip} = -\frac{1}{2} \varepsilon_{ijk} \hat{R}_{mj} \frac{\partial \hat{R}_{mj}}{\partial X_p} \tag{2}$$

Where $\hat{E}_{ij}$ and K_{ip} represent the biot-like translation and curvature tensor.

2.2 Kinetics

The assumption of the micropolar continuum introduces a couple stress along with the classical force stress. Let us denote the elastic energy density as ψ^{elas}, which depends on the strain measures, and define the force stress and couple stress as

$$S_{ij} = \frac{\partial \psi^{\text{elas}}}{\partial \hat{E}_{ij}} \tag{3}$$

$$S^{\mathrm{c}}_{ij} = \frac{\partial \psi^{\mathrm{elas}}}{\partial \hat{K}_{ij}} \tag{4}$$

2.3 Balance Laws

The total energy in the phase field model consists of two parts, namely elastic and fracture. For the micropolar continuum undergoing finite rotation, it has the following form

$$\psi^{\mathrm{elas}} = \hat{\psi}^{\mathrm{elas}}(\hat{E}_{ij}, \hat{K}_{ij}) \tag{5}$$

and

$$\psi^{\mathrm{frac}} = \hat{\psi}^{\mathrm{frac}}(s, g_i) \tag{6}$$

where we have represented the gradient of the phase field variable, $\left(\frac{\partial s}{\partial X_i}\right)$ as g_i.

By taking the energy variation, we can arrive at the governing equations. The balance of linear momentum has the form (neglecting the body force and body couple)

$$\begin{aligned} \frac{\partial(\hat{R}_{ik}S_{kj})}{\partial X_j} &= 0, \text{ on } \Omega \\ \hat{R}_{ik}S_{kj}n_j &= t_i, \text{ on } \Gamma_N \end{aligned} \tag{7}$$

The balance of angular momentum is

$$\begin{aligned} \frac{\partial(\hat{R}_{ik}S^{\mathrm{c}}_{kj})}{\partial X_j} + \varepsilon_{ijk}(\hat{R}S^{c}F^{T})_{kj} &= 0, \text{ on } \Omega \\ \hat{R}_{ik}S^{\mathrm{c}}_{kj}n_j &= t^{\mathrm{c}}_i, \text{ on } \Gamma_N \end{aligned} \tag{8}$$

where t_i and t^{c}_i, represent the components of force traction and couple traction, respectively.

The governing equation corresponding to damage is

$$\frac{\partial}{\partial X_k}\left(\frac{\partial \psi^{\mathrm{frac}}}{\partial g_k}\right) - \frac{\partial \psi}{\partial s} = 0 \tag{9}$$

One can notice that, unlike the classical continuum, angular momentum balance doesn't result in symmetry of the Cauchy stress tensor. Thus, it also needs to be solved to characterize the deformation completely.

3 Numerical Implementation

For the purpose of numerical implementation, we have taken the specialized form of energy density as

$$\begin{aligned} \psi^{\mathrm{elas}} = g(s)(\mu(\hat{E}^{\mathrm{sym}}_{\mathrm{dev}})_{ij}(\hat{E}^{\mathrm{sym}}_{\mathrm{dev}})_{ij} + \\ \mu_c(\hat{E}^{\mathrm{skew}})_{ij}(\hat{E}^{\mathrm{skew}})_{ij} + \frac{\kappa}{2}(\hat{E}_{kk})^2 + \frac{\gamma}{2}\hat{K}_{ij}\hat{K}_{ij}) \end{aligned} \tag{10}$$

and

$$\psi^{\mathrm{frac}} = G_c\left(\frac{3}{8l}(1-s) + \frac{3l}{8}g_i g_i\right). \tag{11}$$

The governing equation corresponding to the damage can be rewritten as,

$$\frac{\partial}{\partial X_i}\left(\frac{3}{4}l^2 g_i\right) - g'(s)\mathcal{J} + \frac{3}{8} = 0. \tag{12}$$

The constant μ_c and γ can be defined in terms of micropolar ratio (Ψ) and bending length scale (l_b) as

$$l_b = \sqrt{\frac{\gamma}{4G}} \tag{13a}$$

$$\gamma = 4Gl_b^2 \tag{13b}$$

$$\mu_c = \frac{\Psi^2}{1-\Psi^2}G \tag{13c}$$

We have used the split proposed by [8] and define the part of the strain energy density contributing to damage as

$$\begin{aligned} \psi^{\mathrm{elas}}_{+} = \mu(\hat{E}^{\mathrm{sym}}_{dev})_{ij}(\hat{E}^{\mathrm{sym}}_{dev})_{ij} + \mu_c(\hat{E}^{\mathrm{skew}})_{ij}(\hat{E}^{\mathrm{skew}})_{ij} \\ + \frac{\kappa}{2}\langle(\hat{E})_{kk}\rangle^2_{+} + \frac{\gamma}{2}\hat{K}_{ij}\hat{K}_{ij} \end{aligned} \tag{14}$$

where $\langle\bullet\rangle_{+} = \frac{1}{2}(\bullet + |\bullet|)$.

Where $\mathcal{J} = \frac{\psi^{\mathrm{elas}}_{+}}{G_c/l}$ is the degrading nondimensionalized strain energy density. To ensure the initial elastic limit, the cohesive fracture model should possess a threshold; therefore, following [4], we introduce the history function as

$$\mathcal{H} = \max_{\tau\in[0,t]}\left(\mathcal{J}_{\mathrm{crit}} + \langle\frac{\mathcal{J}}{\mathcal{J}_{\mathrm{crit}}} - 1\rangle_{+}\right). \tag{15}$$

We write the modified governing equation corresponding to damage as

$$\frac{\partial}{\partial X_i}\left(\frac{3}{4}l^2 g_i\right) - g'(s)\mathcal{H} + \frac{3}{8} = 0. \tag{16}$$

The governing equation has been solved in the framework of the hybrid method proposed by [9]. The update of the displacement, phase field and rotation field has been done similarly to [10].

4 Numerical Examples

To show the applicability of the phase field model for the micropolar continuum, we reproduce the experimental load-displacement plot and also study the effect of the parameters Ψ and l_b on the load-displacement response of concrete specimens.

4.1 Hoover Test

We validate our model by reproducing the experimental load-displacement curve reported in the experimental study done by [11]. The geometry of the problem is shown in Figure 1. The material properties has been taken as $E = 41000$ Mpa, $G_c = 0.05$ N/mm, $\nu = 0.17$ $\psi_{crit} = 0.00024$ N/mm^2.

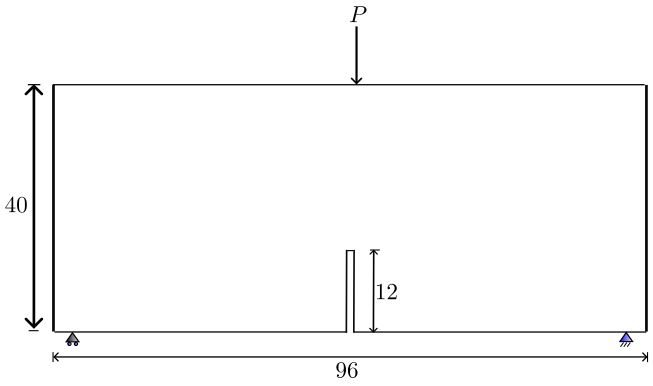

Figure 1: Geometry and boundary conditions of the Hoover test specimen (All dimensions are in mm).

We compare the model's behaviour without micropolar effects with experimental data in the first simulation. The load was applied in the form of incremental displacement of 1×10^{-3} mm per increment till it reached 0.08 mm applied displacement. Figure 2 illustrates the predicted crack path at this final displacement, demonstrating good agreement with experimental observations.

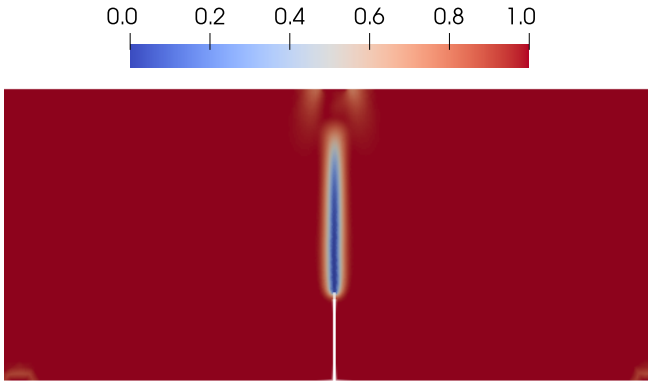

Figure 2: Phase field contour at the applied displacement of 0.08 mm

We also compare the load-displacement response obtained using the numerical simulation in this study with the experimental plot. It shows that the model can predict peak load within the experimental band. We also notice the insensitivity of the model to the length scale $l = 0.85$ mm and $l = 1.05$ mm, attached to the gradient of the phase field. This feature enables the exploration of micropolar continuum parameters on macroscopic responses. We refer to [4] for further details on length scale insensitivity.

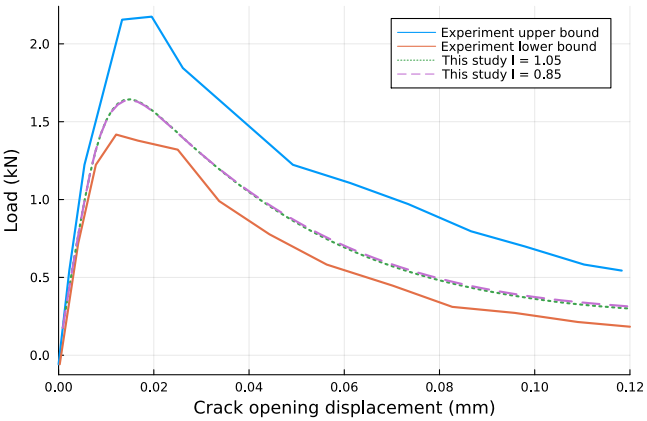

Figure 3: Comparison of load-displacement plot obtained in this study using two different phase field length scale

4.2 Effect of micropolar ratio Ψ

To examine the role of parameters of micropolar continua, we revisit the problem from the previous section. We maintain a constant bend-

ing length scale l_b as 0.01 mm and vary the micropolar ratio. All other material parameters and loading conditions remain identical to those in the previous section.

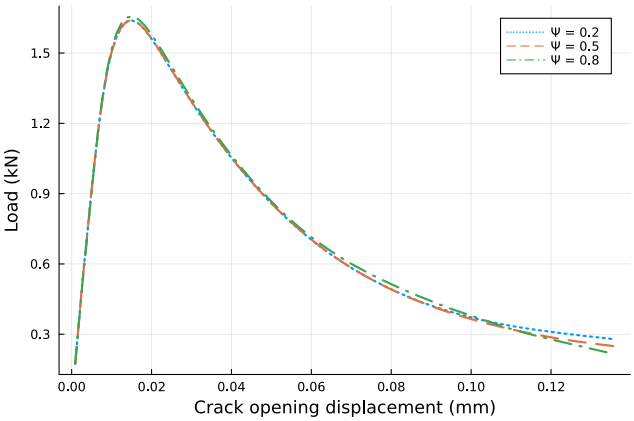

Figure 4: Comparison of load-displacement curve for micropolar ratios of $0.2, 0.5$ and 0.8.

Figure 4 shows the load vs cod plot for three cases of Ψ i.e. $0.2, 0.5$ and 0.8. We observe that the micropolar ratio has a negligible effect on the load-displacement response. This outcome is anticipated, as rotations – primarily induced by shear stress components – are insignificant under mode I loading conditions.

4.3 Effect of bending length scale

We consider the same problem as considered in the previous section. We fix the micropolar ratio Ψ as 0.01 mm and vary the bending length scale. All other material parameters and the loading condition are similar to those in the previous section.

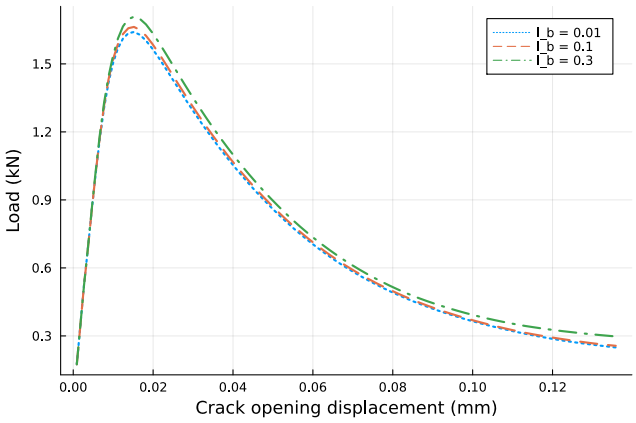

Figure 5: Comparison of load displacement curve for bending length scale of $0.01, 0.1$ and 0.3 mm.

Figure 5 shows the load vs cod plot for three cases of l_b i.e. $0.01, 0.1$ and 0.3. We observe that the bending length scale modifies the peak load. Specifically, peak load increases with the increase in the value of l_b. From the mesoscale perspective, it has been observed that peak load is modified due to the arrangement of the aggregates [12].

5 Conclusion

This study introduces a phase field model for micropolar continua capable of finite rotation of inner structure. We derive governing equations for general finite deformations and employ St. Venant-Kirchhoff constitutive relations for concrete. We recognise their suitability for this material compared to other material models, such as Neo-Hookean models better suited for plastic and rubber-type materials. We apply the model to a concrete boundary value problem, demonstrating its applicability to quasi-brittle materials. Parametric studies reveal that micropolar parameters effectively capture the influence of the material's microstructure, such as aggregate in concrete, and can shed light on experimental scatter arising from mesoscale or microscopic uncertainties. While this work focuses on Mode I fracture, future research should investigate mixed-mode fracture behaviour. Additionally, the model's inherent additional length scale parameter offers the potential for more accurate modelling of size-dependent phenomena.

REFERENCES

[1] A Cemal Eringen. Mechanics of micropolar continua. In *Contributions to Mechanics*, pages 23–40. Elsevier, 1969.

[2] A Cemal Eringen. Theory of thermo-microstretch elastic solids. *International journal of engineering science*, 28(12):1291–1301, 1990.

[3] Ahmed Cemal Eringen. Mechanics of micromorphic materials. In *Applied Mechanics: Proceedings of the Eleventh International Congress of Applied Mechanics Munich (Germany) 1964*, pages 131–138. Springer, 1966.

[4] Hyoung Suk Suh, WaiChing Sun, and Devin T O'Connor. A phase field model for cohesive fracture in micropolar continua. *Computer Methods in Applied Mechanics and Engineering*, 369:113181, 2020.

[5] Pham Hong Cong, Doan Hong Duc, et al. Phase field model for fracture based on modified couple stress. *Engineering Fracture Mechanics*, 269:108534, 2022.

[6] Raymond David Mindlin and HF144513 Tiersten. Effects of couple-stresses in linear elasticity. *Archive for Rational Mechanics and analysis*, 11:415–448, 1962.

[7] Sara Grbčić Erdelj, Gordan Jelenić, and Adnan Ibrahimbegović. Geometrically non-linear 3d finite-element analysis of micropolar continuum. *International journal of solids and structures*, 202:745–764, 2020.

[8] Hanen Amor, Jean-Jacques Marigo, and Corrado Maurini. Regularized formulation of the variational brittle fracture with unilateral contact: Numerical experiments. *Journal of the Mechanics and Physics of Solids*, 57(8):1209–1229, 2009.

[9] Marreddy Ambati, Tymofiy Gerasimov, and Laura De Lorenzis. A review on phase-field models of brittle fracture and a new fast hybrid formulation. *Computational Mechanics*, 55:383–405, 2015.

[10] Ved Prakash, Mohammad Masiur Rahaman, and Debasish Roy. A microstructural defect-orientation informed phase field model. *European Journal of Mechanics-A/Solids*, 109:105472, 2025.

[11] Christian G Hoover, Zdeněk P Bažant, Jan Vorel, Roman Wendner, and Mija H Hubler. Comprehensive concrete fracture tests: Description and results. *Engineering fracture mechanics*, 114:92–103, 2013.

[12] Yang Xia, Wenan Wu, Yongtao Yang, and Xiaodong Fu. Mesoscopic study of concrete with random aggregate model using phase field method. *Construction and Building Materials*, 310:125199, 2021.